

Growth and characteristics of GaInN/GaN multiple quantum well light-emitting diodes

Wonseok Lee,¹ Min-Ho Kim,² Di Zhu,³ Ahmed N. Noemaun,⁴ Jong Kyu Kim,⁵ and E. F. Schubert^{4,a)}

¹*Future Chips Constellation and Engineering Science Program, Rensselaer Polytechnic Institute, Troy, New York 12180, USA*

²*Samsung LED, Suwon 443-743, South Korea*

³*Future Chips Constellation and Department of Physics, Applied Physics, and Astronomy, Rensselaer Polytechnic Institute, Troy, New York 12180, USA*

⁴*Future Chips Constellation and Department of Electrical, Computer, and Systems Engineering, Rensselaer Polytechnic Institute, Troy, New York 12180, USA*

⁵*Department of Materials Science and Engineering, Pohang University of Science and Technology, Pohang 790-784, South Korea*

(Received 21 October 2009; accepted 25 January 2010; published online 16 March 2010)

We demonstrate GaInN multiple quantum well (MQW) light-emitting diodes (LEDs) having ternary GaInN quantum barriers (QBs) instead of conventional binary GaN QBs for a reduced polarization mismatch between QWs and QBs and an additional separate confinement of carriers to the MQW active region. In comparison with GaInN LEDs with conventional GaN QBs, the GaInN/GaN LEDs show a reduced blueshift of the peak wavelength with increasing injection current and a reduced forward voltage. In addition, we investigate the density of pits emerging on top of the MQW layer that are correlated with V-defects and act as a path for the reverse leakage current. The GaInN/GaN MQW structure has a lower pit density than the GaInN/GaN MQW structure as well as a lower reverse leakage current. Finally, the GaInN/GaN MQW LEDs show higher light output power and external quantum efficiency at high injection currents compared to the conventional GaInN/GaN MQW LEDs. We attribute these results to the reduced polarization mismatch and the reduced lattice mismatch in the GaInN/GaN MQW active region. © 2010 American Institute of Physics. [doi:10.1063/1.3327425]

I. INTRODUCTION

III-nitride-based high-brightness light-emitting diodes (LEDs) operating at visible wavelengths have been advanced by metal-organic vapor-phase epitaxy (MOVPE) growth techniques. The emission wavelength and efficiency of GaN-based LEDs grown on *c*-plane sapphire substrates are influenced by a strong internal electric field, on the order of MV/cm, induced by spontaneous and piezoelectric polarization in the multiple quantum well (MQW) active region. In case of a typical MQW active region, in which GaInN QWs are sandwiched between GaN quantum barriers (QBs), the piezoelectric polarization is known to be dominant due to the large lattice mismatch between GaInN QWs and the GaN confinement layer.¹ Spontaneous polarization occurs in the III-nitride wurtzite crystal even if there is no strain present. The strong polarization-induced electric field causes spatial separation of electron and hole wave functions inside the QWs, resulting in a reduced internal quantum efficiency. At low injection currents, the electric field and the associated quantum-confined Stark effect (QCSE) in a GaInN/GaN MQW structure cause a redshift of the electroluminescence (EL) peak wavelength compared to a QCSE-free MQW layer. Furthermore, the peak-emission wavelength shifts back to the blue with increasing injection current. As a result,

the spectrum, correlated color temperature, and the color rendering index of phosphor-converted white LEDs vary with injection current.

It has been proposed and demonstrated that the internal electric fields can be considerably reduced by controlling the polarization and the strain in the active region,²⁻⁸ and by using alternative non-*c*-polar orientations of native substrates.^{9,10} In addition, it has been reported that the polarization-induced electric field causes electron leakage out of the active region at high drive currents, and thus reduces the LED efficiency at high currents.² Instead of conventional GaN QBs, fully polarization-matched (100%) AlGaInN and AlInN QBs as well as partially polarization-matched (<100%) GaInN QBs have been proposed to reduce the efficiency droop by enabling independent control over interface polarization charges as well as bandgap.^{2,3} However, it is difficult to grow high-quality AlGaInN and AlInN QBs with high aluminum (Al) and indium (In) compositions that are required for simultaneous and complete matching of polarization charges with GaInN QWs. As an alternative, even Al-free Ga_{1-y}In_yN QBs can reduce the polarization mismatch with respect to the Ga_{1-x}In_xN QWs ($x > y$). The reduction in polarization mismatch between QW and QB of Ga_{0.80}In_{0.20}N/Ga_{0.90}In_{0.10}N MQW structures compared with Ga_{0.80}In_{0.20}N/GaN MQW structure is 50%. It has been shown by simulations that, at high currents, GaInN/GaN MQW structures give a similarly increased light output

^{a)}Author to whom correspondence should be addressed. Electronic mail: efschubert@rpi.edu.

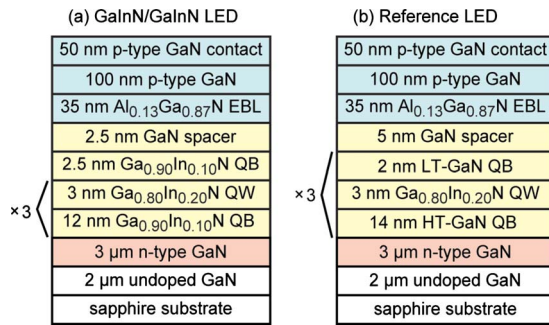


FIG. 1. (Color online) Schematic epitaxial structures of (a) GaInN/GaN MQW LED (GaInN/GaN LED) and (b) GaInN/GaN MQW LED (reference LED). In both structures, the growth conditions are the same for all layers except the QBs.

power (LOP) and decreased efficiency droop as GaInN/AlGaInN MQW LED structures.¹¹ The polarization-matched GaInN QBs have an additional separate confinement of carriers to the active region enabled by the reduced bandgap of the QBs.¹¹

In this work, we present a systematic study on the design, growth, and characterization of the GaInN/GaN MQW LEDs to investigate the effect of polarization charges at the interface between QWs and QB on the performance of the LEDs. The structural properties of GaInN/GaN MQW structures are thoroughly studied by high resolution x-ray diffraction (XRD) and atomic force microscopy (AFM). Also, the correlation between the structural properties and the electrical performance and the optical properties of GaInN/GaN MQW LEDs and GaInN/GaN MQW LEDs are discussed. The reduced polarization mismatch in the GaInN/GaN MQW LEDs is found to result in a reduced blueshift of the EL peak wavelength with increasing current, and a reduced forward voltage. In addition, the GaInN/GaN MQW shows a lower pit density and a reduced reverse leakage current. Finally, the GaInN/GaN MQW LEDs are demonstrated to have an improved LOP and external quantum efficiency (EQE).

II. EXPERIMENTAL PROCEDURES

The epitaxial structures of the LEDs were grown on *c*-plane (0001) sapphire substrates by using a single-wafer Aixtron MOVPE system. The LED epitaxial structures consist of an undoped GaN layer (2 μm) grown on a low-temperature GaN buffer layer (30 nm), a Si-doped n-type GaN layer (3 μm), a three-period GaInN/GaN (3 nm/12 nm) or GaInN/GaN (3 nm/16 nm) MQW active region, a undoped GaN spacer layer, a Mg-doped p-type $\text{Al}_{0.13}\text{Ga}_{0.87}\text{N}$ electron blocking layer (EBL) (35 nm), a Mg-doped p-type GaN hole injection layer (100 nm), and a heavily Mg-doped GaN contact layer (50 nm) as shown in Fig. 1. We call the structure shown in Fig. 1(a) the “GaInN/GaN LED” and the structure shown in Fig. 1(b) the “reference LED.” For the GaN QBs in Fig. 1(b), a 2 nm thick GaN layer (LT-GaN QB) was first grown at 720 $^{\circ}\text{C}$ which is same growth temperature (corrected surface temperature for the emissivity of the wafer) used for QWs to protect the GaInN QW from thermal decomposition during the ramping up of the growth temperature. Then, a 14 nm thick GaN QB (HT-GaN QB) was grown

at 790 $^{\circ}\text{C}$ to ensure good crystal quality. However, GaInN QBs in Fig. 1(a) were grown without a GaN protection layer between QWs and QBs and at a lower growth temperature than the HT-GaN QBs. The GaInN QBs are thinner than the GaN QBs in order to maintain good crystal quality of the QBs. The target In composition in the GaInN QWs and GaInN QBs is 20% (to emit blue light) and 10% (to have reduced polarization mismatch between QW and QB), respectively. We use a 2.5 nm thick GaInN layer as the last QB followed by a 2.5 nm thick GaN spacer layer for the GaInN/GaN LED. We use a 2 nm thick LT-GaN layer as the last QB followed by a 5 nm thick GaN spacer layer for the reference LED. In both structures, the growth conditions are the same for all layers except the QBs.

As a first indication of the material quality, the surface morphology is mirror-like for both samples. After the wafers are annealed at 800 $^{\circ}\text{C}$ for 1 min, under N_2 ambient, for p-type GaN doping activation, the two LED structures are processed into $300 \times 300 \mu\text{m}^2$ LED devices by using standard LED fabrication techniques. Ti/Al/Ti/Au and NiZn/Ag metal schemes are used for n-type and p-type Ohmic contact, respectively. The structural quality and thickness of the active region are investigated by XRD and AFM. Current-voltage (*I*-*V*) characteristics are performed in pulsed mode with 20 μs pulse width and a 1% duty cycle to eliminate joule heating. The LOP is measured from the light emission through the sapphire substrate onto a Si photodiode. EL is measured by a high-resolution spectrometer, collecting photons emitted from the LED wafers by an optical fiber. All devices on the wafer are electrically measured by four probes to get an accurate value of the forward voltage.

III. RESULTS AND DISCUSSION

In order to estimate the electric field in the QWs of the two LED structures shown in Fig. 1, simulations are performed using APSYS modeling software. APSYS uses a combination of different carrier transport models. For the n-type and p-type confinement layers, a drift-diffusion model is used to calculate the current. In the MQW region, a thermionic emission model is used. To calculate carrier concentrations at various points in the QWs and the surrounding QBs, APSYS integrates the electron and hole wave functions of the various calculated energy levels in the QW and QB. Thus APSYS incorporates tunneling effects into the carrier transport model. Commonly accepted parameters are used in the simulations.¹² The spontaneous and piezoelectric polarization fields yield charges at the interface of QWs and QBs. The spontaneous and piezoelectric polarization elementary charge densities of 3.5×10^{12} and $6.5 \times 10^{12} \text{ cm}^{-2}$ are used for the GaInN/GaN LED and the GaInN/GaN LED, respectively. These elementary charge densities correspond to 50% of the theoretically predicted values.¹³ This is done to facilitate the numerical convergence of APSYS modeling. In both structures, the QWs, the last QB, and the spacer layer are undoped. A residual donor concentration of $5 \times 10^{16} \text{ cm}^{-3}$ is used in the simulation for the undoped layers. The Si doped QBs have the extrinsic donor concentration of $2 \times 10^{18} \text{ cm}^{-3}$. The band offsets for the AlGaIn/GaN and the

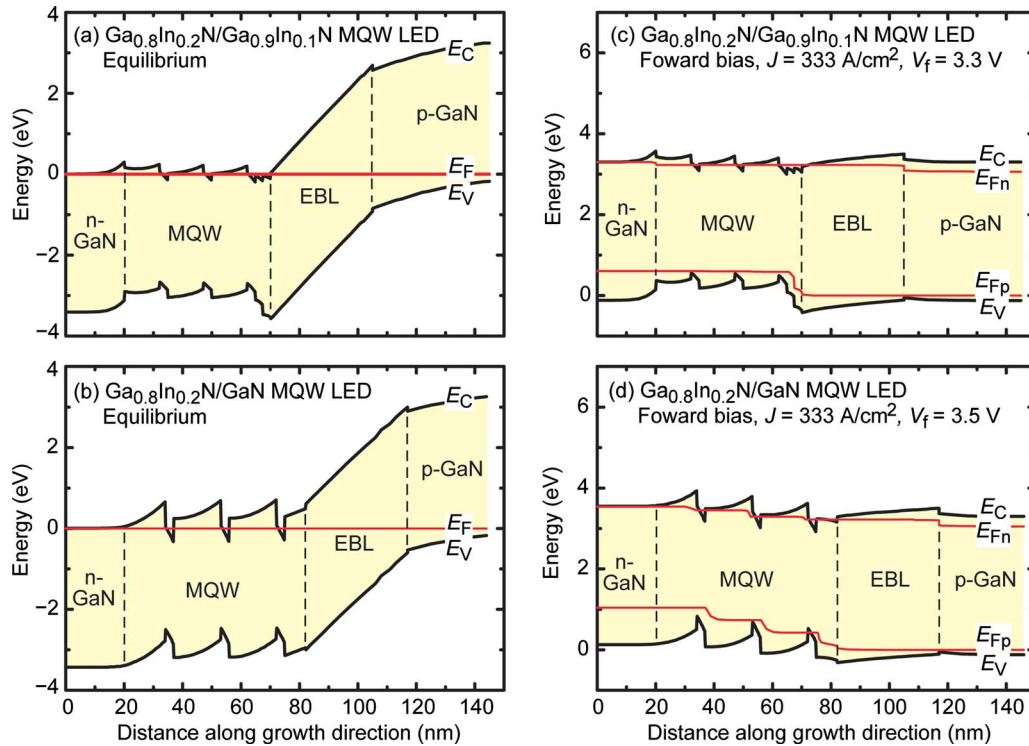


FIG. 2. (Color online) Calculated energy band diagrams of the GaInN/GaInN MQW LED and the GaInN/GaN MQW LED under equilibrium and under forward bias.

GaN/GaInN heterostructures are chosen to be 50%, that is $\Delta E_C/\Delta E_g = 50\%$, and $\Delta E_C = \Delta E_V$.

Figure 2 shows the calculated band diagrams of the GaInN/GaInN MQW LED and GaInN/GaN MQW LED at equilibrium and under a forward-bias condition. Under the forward-bias condition, the current density is 333 A/cm². For the GaInN/GaInN MQW structure, the polarization sheet charges at the interfaces between GaInN QWs and GaInN QBs are reduced as compared to the reference LED. The internal electric field (slope of band edges) in the QWs and QBs is reduced as well. In addition, the reduced height of the QBs is more favorable to electron and hole flow, potentially resulting in a low forward voltage.

We note that for the reference LED structure, under the high forward bias, the conduction band on the p-side is lower than on the n-side. We also note that for the GaInN/GaInN MQW LED structure, under the high forward bias, the conduction band on the p-side is higher than that on the n-side making it more difficult for electrons to reach the p-side. As a result, the electron leakage over the EBL is reduced.

Figure 3 plots the calculated electric fields in the last QW layer of the GaInN/GaInN LED and reference LED. The electric fields at different forward currents are calculated and plotted by using the appropriate slope of the band diagram. The electric field in the QW layer of the GaInN/GaInN LED structure is much less than that of the reference LED structure, indicating a reduced polarization mismatch between QWs and QBs by using the GaInN QBs. Furthermore, given the reduced field, we expect that the GaInN/GaInN LED has a much smaller shift of the peak wavelength than the reference LED when the injection current is increased.

Figure 4 shows the measured and simulated XRD ω - 2θ

scans of the GaInN/GaInN LED and reference LED wafer. The two measured XRD curves exhibit quite different shapes of the satellite peaks of the MQW and the spacing of the peaks related to the superlattice fringes are different because of a higher total In content and thinner GaInN QBs in the GaInN/GaInN active region. The satellite peaks of the reference LED structure are clearly seen up to the fifth order, thus confirming that the interfaces between GaInN QWs and GaN QBs are well defined. However, the satellite peaks of the GaInN/GaInN LED structure are less distinct and broader than those of the reference LED structure. In addition, the intensity of the satellite peaks of the GaInN/GaInN LED structure is lower than that of the reference LED structure. These differences are attributed to the greater similarity between GaInN QWs and GaInN QBs, as compared to GaInN QWs and GaN QBs. This is confirmed by the simulated XRD curve as shown in the Fig. 4(b).

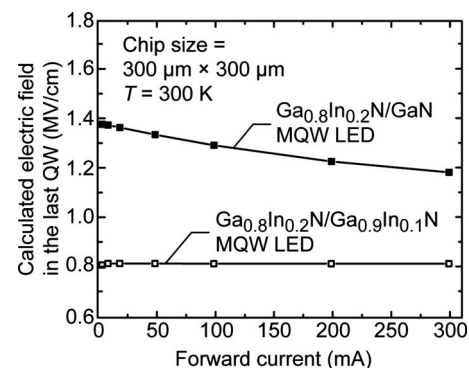


FIG. 3. Calculated electric fields in the last QW layer of the GaInN/GaInN MQW LED and GaInN/GaN MQW LED structures as a function of the injected forward current.

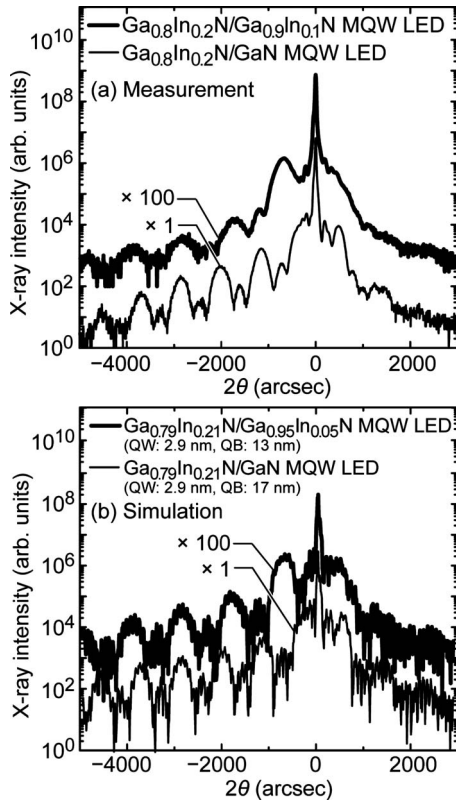


FIG. 4. (a) Measured and (b) simulated XRD ω - 2θ scans using triple-axis optics on blue LED structures with GaInN/GaInN and GaInN/GaN MQWs.

Figure 5 shows I - V characteristics of the fabricated GaInN/GaInN LED and reference LED. The turn-on and forward voltages for the GaInN/GaInN LED are lower than those for the reference LED. Under a 300 mA current injection, the forward voltages are 4.1 and 4.6 V for the GaInN/GaInN LED and reference LED, respectively. Also, the series resistance of GaInN/GaInN LED is lower than that of the reference LED. The improved electrical properties of the GaInN/GaInN LEDs can be attributed to the reduced energy barriers in QBs for both electron and hole transport resulting from the reduction of polarization mismatch and sheet charges at the interfaces of QBs and QWs in the active region as shown in Fig. 2. The experimentally found reduction of the forward voltage is qualitatively consistent with the

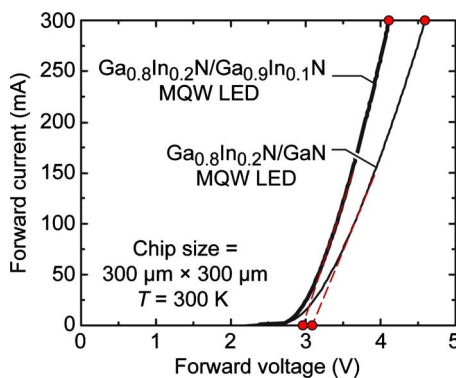


FIG. 5. (Color online) Measured I - V characteristics of the blue LEDs with GaInN/GaInN and GaInN/GaN MQWs.

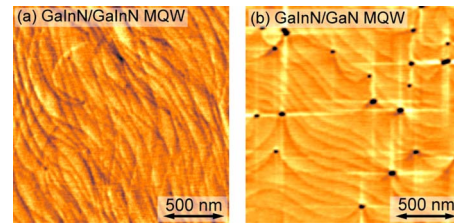


FIG. 6. (Color online) AFM images of (a) GaInN/GaInN MQW and (b) GaInN/GaN MQW structures with scan area of $2 \times 2 \mu\text{m}^2$. The structures were grown up to the last QB without EBL and p-type layers.

theoretical modeling which also reveals a 0.2 V reduction in the forward voltage for the GaInN/GaInN LED structure.

Figure 6 shows the AFM images of the GaInN/GaInN MQW and GaInN/GaN MQW with a scan area of $2 \times 2 \mu\text{m}^2$. In order to observe the surface morphology of the active region, the MQW samples were grown up to the last QB without p-type layers. A high density of dark pits is observed in the GaInN/GaN MQW structure. The density of these defects is estimated as $5.3 \times 10^8 \text{ cm}^{-2}$. The GaInN layer or GaInN/GaN MQW often show, depending on thickness and composition of GaInN, a surface morphology with a high density of pits correlated with the V-defects (also called inverted hexagonal pyramids), which have been proven to be associated with threading dislocations at their apices.^{14–17} Because of the reduced lattice mismatch between $\text{Ga}_{0.80}\text{In}_{0.20}\text{N}$ QWs and $\text{Ga}_{0.90}\text{In}_{0.10}\text{N}$ QBs, the $\text{Ga}_{0.80}\text{In}_{0.20}\text{N}/\text{Ga}_{0.90}\text{In}_{0.10}\text{N}$ MQW active region presumably has a lower strain than the $\text{Ga}_{0.80}\text{In}_{0.20}\text{N}/\text{GaN}$ MQW active region. In addition, possible generation of new dislocations in the GaInN/GaN active region due to the large lattice mismatch between GaInN QW and GaN QB is likely to be reduced between GaInN QW and GaInN QB.

Figure 7 shows the typical reverse I - V characteristics of both types of LEDs measured at room temperature. The reverse current of the GaInN/GaInN LED is significantly reduced, which is presumably due to the improved morphology of MQW active region as shown in Fig. 6. It has been reported that the V-defects and the associated screw and mixed dislocations are responsible for the large leakage currents observed in LED structures.^{18,19} Therefore, we attribute the much lower reverse leakage current in the GaInN/GaInN LED to the reduced dislocation-related pit density.

Next, the electro-optical properties of the LEDs with dif-

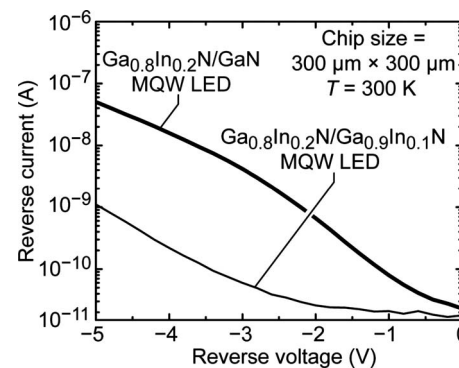


FIG. 7. Reverse current vs reverse voltage curve of GaInN/GaInN MQW LED and GaInN/GaN MQW LED.

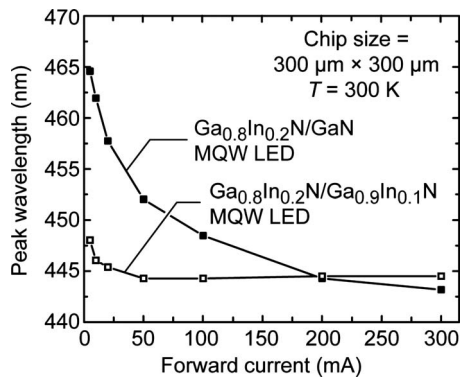


FIG. 8. Measured peak wavelength vs forward current from 300 K EL measurement of blue LEDs with GaInN/GaN and GaInN/GaN MQW active region.

ferent QBs are compared. Figure 8 displays the change of peak wavelength of the EL spectrum for various injection currents. First, at low injection current, the peak wavelength for the GaInN/GaN LED is much shorter than that for the reference LED due to a reduced polarization-induced electric field in the active region. Second, the blueshift of EL peak for the GaInN/GaN LED is much reduced as compared to that for the reference LED, consistent with our APSYS simulation. As the current increases from 5 to 300 mA, the wavelength shifts are 3.5 and 21.0 nm for the GaInN/GaN LED and reference LED, respectively. The remarkable reduction of blueshift for the GaInN/GaN LED suggests the mitigation of QCSE by the reduction of the polarization-induced internal electric field in the QWs.

Figures 9(a) and 9(b) show the measured LOP and the corresponding normalized EQE as a function of the forward current for the GaInN/GaN LED and reference LED. As

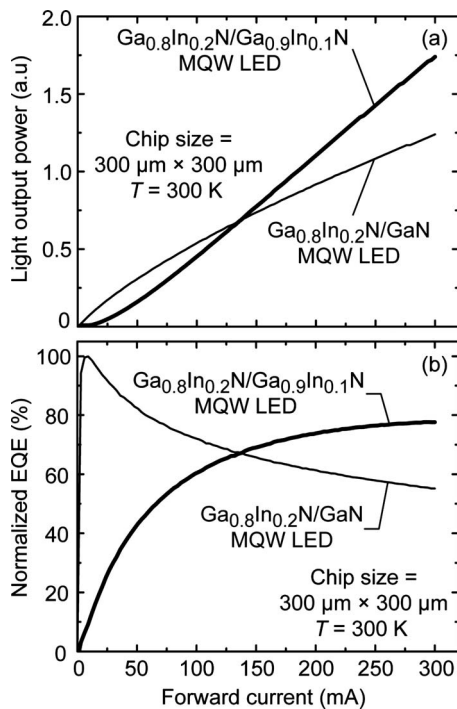


FIG. 9. (a) Measured LOP and (b) normalized EQE of the GaInN/GaN MQW LED and GaInN/GaN MQW LED as function of forward current.

shown in Fig. 9(a), in the low forward-current regime, the LOP of the GaInN/GaN LED is lower than that with GaInN/GaN MQW. However, in the high current regime, the LOP of the GaInN/GaN LED overcomes that of the reference LED. As shown in Fig. 9(b), the reference LED has a sharp peak in EQE, which occurs at 10 mA. The EQE rapidly decreases as the forward current increases to 300 mA, resulting in the typical efficiency droop of the conventional LEDs. The calculated efficiency droop is 45% by using a droop definition of $(\eta_{\text{peak}} - \eta_{300 \text{ mA}}) / \eta_{\text{peak}}$. However, the GaInN/GaN LED shows a different dependency of the EQE on the forward current. The EQE gradually increases in the low current regime, and the EQE curve is saturating in the high current regime. For the GaInN/GaN MQW LED, the efficiency-versus-current curve continuously increases and does not have a peak in the measured current range. In the high current regime, the EQE of the GaInN/GaN LED is higher than that of the reference LED. The higher output power is consistent with polarization-matched LED structures reducing droop and electron leakage.

IV. CONCLUSIONS

We have presented GaInN LEDs with GaInN QBs, rather than conventional GaN QBs, to reduce polarization mismatch between the GaInN QWs and the QBs. The EL spectra of the GaInN/GaN LED show much less blueshift with increasing injection current as compared to the GaInN/GaN reference LED. The forward voltage is reduced in the GaInN/GaN LED due to reduced energy barriers for electron and hole transport. In addition, the pit density in the GaInN/GaN MQW is much reduced and correlated with a reduced reverse leakage current in the GaInN/GaN LED. Furthermore, the LOP and EQE of the GaInN/GaN LED are much improved over those of the GaInN/GaN reference LED. These results are attributed to the reduction of polarization mismatch and the reduction of lattice mismatch in the MQW active region by using GaInN QBs.

ACKNOWLEDGMENTS

The authors gratefully acknowledge support by the Samsung LED, New York State, Sandia National Laboratories, Department of Energy, National Science Foundation, and Crystal IS.

¹E. F. Schubert, *Light-Emitting Diodes*, 2nd ed. (Cambridge University Press, Cambridge, UK, 2006).

²M.-H. Kim, M. F. Schubert, Q. Dai, J. K. Kim, E. F. Schubert, J. Piprek, and Y. Park, *Appl. Phys. Lett.* **91**, 183507 (2007).

³M. F. Schubert, J. Xu, J. K. Kim, E. F. Schubert, M. H. Kim, S. Yoon, S. M. Lee, C. Sone, T. Sakong, and Y. Park, *Appl. Phys. Lett.* **93**, 041102 (2008).

⁴J. Xu, M. F. Schubert, A. N. Noemaun, J. K. Kim, E. F. Schubert, M. H. Kim, H. J. Chung, S. Yoon, C. Sone, and Y. Park, *Appl. Phys. Lett.* **94**, 011113 (2009).

⁵A. Knauer, H. Wenzel, T. Kolbe, S. Einfeldt, M. Weyers, M. Kneissl, and G. Tränkle, *Appl. Phys. Lett.* **92**, 191912 (2008).

⁶J.-H. Ryou, W. Lee, J. Limb, D. Yoo, J. P. Liu, R. D. Dupuis, Z. H. Wu, A. M. Fischer, and F. A. Ponce, *Appl. Phys. Lett.* **92**, 101113 (2008).

⁷C.-Y. Wang, L.-Y. Chen, C.-P. Chen, Y.-W. Cheng, M.-Y. Ke, M.-Y. Hsieh, H.-M. Wu, L.-H. Peng, and J. Huang, *Opt. Express* **16**, 10549 (2008).

⁸T. Asano, T. Tojyo, T. Mizuno, M. Takeya, S. Ikeda, K. Shibuya, T. Hino, S. Uchida, and M. Ikeda, *IEEE J. Quantum Electron.* **39**, 135 (2003).

- ⁹K. Iso, H. Yamada, H. Hirasawa, N. Fellows, M. Saito, K. Fujito, S. P. DenBaars, J. S. Speck, and S. Nakamura, *Jpn. J. Appl. Phys., Part 2* **46**, L960 (2007).
- ¹⁰M. Funato, M. Ueda, Y. Kawakami, Y. Narukawa, T. Kosugi, M. Takahashi, and T. Mukai, *Jpn. J. Appl. Phys., Part 2* **45**, L659 (2006).
- ¹¹M.-H. Kim, W. Lee, D. Zhu, M. F. Schubert, J. K. Kim, E. F. Schubert, and Y. Park, *IEEE J. Sel. Top. Quantum Electron.* **15**, 1122 (2009).
- ¹²F. Bernardini, in *Nitride Semiconductor Devices: Principles and Simulation*, edited by J. Piprek (Wiley, New York, 2007), pp. 49–67.
- ¹³F. Bernardini, V. Fiorentini, and D. Vanderbilt, *Phys. Rev. B* **56**, R10024 (1997).
- ¹⁴X. H. Wu, C. R. Elsass, A. Abare, M. Mack, S. Keller, P. M. Petroff, S. P. DenBaars, J. S. Speck, and S. J. Rosner, *Appl. Phys. Lett.* **72**, 692 (1998).
- ¹⁵Y. Chen, T. Takeuchi, H. Amano, I. Akasaki, N. Yamada, Y. Kaneko, and S. Y. Wang, *Appl. Phys. Lett.* **72**, 710 (1998).
- ¹⁶I.-H. Kim, H.-S. Park, Y.-J. Park, and T. Kim, *Appl. Phys. Lett.* **73**, 1634 (1998).
- ¹⁷D. Cherns, S. J. Henley, and F. A. Ponce, *Appl. Phys. Lett.* **78**, 2691 (2001).
- ¹⁸X. A. Cao, J. A. Teetsov, F. Shahedipour-Sandvik, and S. D. Arthur, *J. Cryst. Growth* **264**, 172 (2004).
- ¹⁹D. S. Li, H. Chen, H. B. Yu, H. Q. Jia, Q. Huang, and J. M. Zhou, *Appl. Phys. Lett.* **96**, 1111 (2004).